Nucleus-nucleus fusion energy thresholds and the adiabatic fusion potential

K. Siwek-Wilczyńska
Institute of Experimental Physics, Warsaw University, PL-00-681 Warsaw, Poland

J. Wilczyński
Institute for Nuclear Studies, PL-05-400 Otwock-Świerk, Poland

(Received 26 February 2001; published 6 July 2001)

Experimental values of fusion energy thresholds, defined as energies at which the fusion cross section equals to the *s*-wave absorption cross section, are compared with barrier heights calculated assuming the adiabatic fusion potential with the nuclear part of the Woods-Saxon shape and parameters unambiguously determined by the liquid-drop-model contact force and the ground-state fusion *Q* value. Predictions of the ''capture'' cross sections in collisions of very heavy systems used to produce new superheavy elements are discussed.

DOI: 10.1103/PhysRevC.64.024611 PACS number(s): 25.70.Jj

I. INTRODUCTION

Nucleus-nucleus fusion excitation functions can be quite well reproduced and understood in terms of the coupled-channels calculations involving coupling to various collective states, effectively enhancing the fusion probability at sub-barrier energies. (See recent review article [1], and references therein.) However, predictive power of the coupled-channels calculations is somewhat limited, especially for heavy systems, for which a very large number of channels with unknown coupling constants should be included. Therefore, for practical purposes such as predictions of fusion cross sections for very heavy systems, the use of macroscopic dynamical models may be useful. It should be noted that coexistence of fusion barriers of different height, the phenomenon naturally present in the coupled-channels calculations, has its classical equivalent in macroscopic models extended by inclusion of thermal and/or shape fluctuations. In the macroscopic description, the fluctuational spreading of trajectories in the configurational space (with an individual barrier height for each trajectory) also leads to a distribution of the fusion barriers.

In this paper we analyze existing data on fusion excitation functions from the point of view of determination of fusion energy thresholds which can be identified with the lowest barriers in the fusion barrier distributions. We also attempt to predict these lowest, adiabatic barriers using a simple nucleus-nucleus fusion potential. It is shown that the experimental fusion thresholds agree very well with the barrier heights calculated with the proposed potential. Moreover, the measured and calculated barriers show close correlation in isotopic nuclear structure effects which seem to modulate the barrier heights.

Our analysis of the correlation between the experimental and calculated fusion and/or capture energy thresholds extends to as heavy systems as ^{40}Ca+ ^{194}Pt (fusion) and ^{58}Fe + ^{209}Pb (capture). This correlation can be extrapolated to still heavier systems, thus providing predictions of the energy thresholds for capture processes in reactions which may be used in future experiments aimed to synthesize new superheavy elements.

II. FUSION ENERGY THRESHOLDS

As was demonstrated by Rowley, Satchler, and Stelson [2], fusion-barrier distributions can be deduced from precisely measured fusion excitation functions by taking the double derivative of the product of the cross section multiplied by energy $d^2(\sigma E)/dE^2$. In most of the studied reactions, the deduced fusion-barrier distributions extend over a range of 5–15 MeV. The low-energy edge in the barrier distributions, ''the lowest barrier,'' is a quantity difficult to determine precisely, but important from a practical point of view, especially for very heavy systems. Location of this ''lowest barrier'' tells us where the onset of above-the-barrier fusion processes is and therefore this energy is a good reference point, which we can call an effective fusion-energy threshold for a given nucleus-nucleus system.

Since extraction from data of the fusion-barrier distributions and determination of ''the lowest barrier'' require precise measurements of the fusion cross sections at the lowest energies, a procedure performed so far only for selected systems, we propose an alternative, easier to apply definition of the fusion-energy threshold which turns out to give threshold values almost exactly coinciding with those resulting from the original definition of ''the lowest barrier.'' We propose to use the following operational definition of the fusion energy threshold: This threshold is the energy $E=E_{\rm thr}$ at which the measured fusion cross section is equal to the *s*-wave absorption cross section

$$\sigma_{\rm fus}=\pi\lambda\!\!\!^{-2}=\frac{\pi\hbar^2}{2\mu E_{\rm thr}}, \tag{1}$$

where $\lambda\!\!\!^{-}$ is the wavelength of the fusing system and μ its reduced mass. Note that in semi-classical language, $\pi\lambda\!\!\!^{-2}$ is a ''minimum portion'' of above-the-barrier fusion cross section and therefore seems to be a quantity appropriate for consistent definition of the easy-to-determine fusion energy threshold.

Using as an example the fusion excitation functions for the ^{40}Ca+ ^{192}Os and ^{40}Ca+ ^{194}Pt reactions measured by Bierman *et al.* [3], we demonstrate in Fig. 1 that our criterion

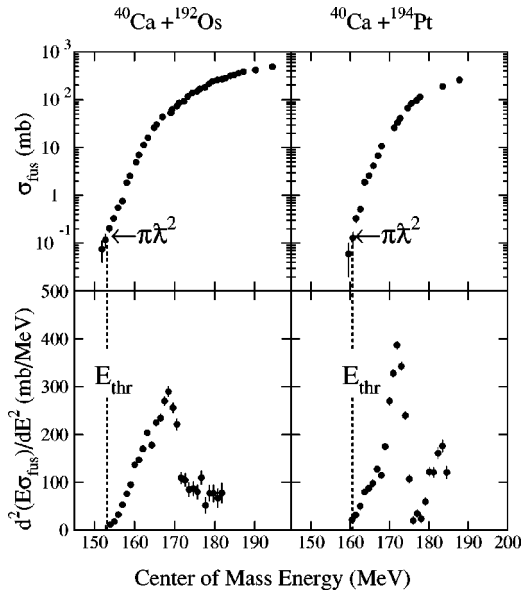

FIG. 1. Illustration of the criterion used for determination of the fusion energy thresholds using the example of fusion excitation functions (top) and deduced fusion barrier distributions (bottom) for the ^{40}Ca+ ^{192}Os and ^{40}Ca+ ^{194}Pt reactions measured by Bierman and co-workers [3]. Data points are redrawn from Fig. 5 of Ref. [3]. Horizontal arrows indicate calculated values of the *s*-wave absorption cross section $\pi\lambda\!\!\!^{-2}$. The corresponding fusion energy thresholds $E_{\rm thr}$ are indicated by vertical dashed lines. They coincide with the low-energy edge of the fusion barrier distributions.

defined by Eq. (1) returns values of $E_{\rm thr}$ which can indeed be identified with ''the lowest barriers'' within the fusion-barrier distributions. We have checked that this is the case in all other reactions taken for our analysis.

In Table I, we list all the reactions for which we have determined the ''experimental'' values of the fusion and/or capture energy threshold $E_{\rm thr}$ with the use of Eq. (1). The corresponding values of the *s*-wave absorption cross section $\pi\lambda\!\!\!^{-2}$ are also listed. Fusion and/or capture excitation functions for about 50 systems, taken from Refs. [3–18] have been used. Apart from the capture data for the heaviest systems [17,18], for all these reactions the excitation functions were measured with high precision and they are known at least down to the threshold limit given by Eq. (1), which for heavy systems is of the order of 0.1 mb. However, light systems and also some heavier but very asymmetric systems involving light projectiles of $A<28$ are not included. This limitation is dictated by the macroscopic approach used in our interpretation of the fusion energy thresholds.

In the following section we give a prescription for a simple nucleus-nucleus fusion potential. The fusion barriers calculated with this potential will be compared with the experimental fusion energy thresholds listed in Table I.

III. THE ADIABATIC FUSION POTENTIAL

A. Nuclear potential

In the macroscopic approach, the potential energy of a nucleus-nucleus system undergoing fusion is usually considered in the configuration space representing particular choice of shape parametrization. For determination of the *adiabatic* nucleus-nucleus fusion potential, we avoid the question of assuming specific shape parametrization. Instead, following the idea of Refs. [19,20], we use only the known characteristics of the system at the onset of nuclear interaction (contact force) and in the final state of the equilibrated compound nucleus. Smooth interpolation between these two reference points is done essentially without free parameters assuming that the effective one-dimensional potential has the Woods-Saxon shape

$$V_n(r)=\frac{-V_0}{1+\exp\left(\dfrac{r-R_0}{a}\right)}. \tag{2}$$

The depth of the nuclear potential V_0 is determined by the ground-state energy of the compound nucleus (with its intrinsic Coulomb energy C_{cn} and shell correction S_{cn} subtracted) taken relative to the sum of the ground-state energies of the two separated nuclei, also with subtracted intrinsic Coulomb energies C_1 and C_2, but shell corrections included:

$$V_0=(M_1+M_2-M_{cn})c^2+C_{cn}-C_1-C_2+S_{cn}, \tag{3}$$

where M_1, M_2, and M_{cn} are the ground state masses and

$$C_{cn}-C_1-C_2=C_0 = 0.7054\left[\frac{(Z_1+Z_2)^2}{(A_1+A_2)^{1/3}}-\frac{Z_1^2}{A_1^{1/3}}-\frac{Z_2^2}{A_2^{1/3}}\right]\text{MeV}. \tag{4}$$

Here, the Coulomb energy constant is taken from the standard liquid-drop-model fit to nuclear masses [21]. The shell correction S_{cn} in Eq. (3), which we take from Ref. [22], has to be subtracted from the ground state energy of the compound nucleus because it produces only a local dip (near the equilibrium shape) in the flat landscape of the nuclear potential energy represented by the inner part of the Woods-Saxon potential.

The diffuseness parameter a in Eq. (2) is determined by the strength of the nucleus-nucleus contact force [23] at the touching distance $R_0=R_1+R_2$, calculated in frame of the liquid-drop model

$$\left(\frac{dV_n}{dr}\right)_{r=R_0}=\frac{V_0}{4a}=4\pi\gamma\frac{R_1R_2}{R_1+R_2}, \tag{5}$$

where

$$\gamma=0.9516\left[1-1.7826\left(\frac{N-Z}{A}\right)^2\right]\text{MeV/fm}^2 \tag{6}$$

is the value of the surface tension coefficient [21] of the combined system with the number of neutrons $N=N_1+N_2$

TABLE I. Fusion energy thresholds $E_{\rm thr}$ deduced from experimental fusion excitation functions using the criterion of the *s*-wave absorption cross section $\sigma(l=0)=\pi\lambda\!\!\!^{-2}$, compared with the fusion barrier heights calculated with the adiabatic fusion potential $B_{\rm adiab}$ and with the Bass potential $B_{\rm Bass}$.

Reaction	Ref.	$\sigma(l=0)$ (mb)	$E_{\rm thr}$ (MeV)	$B_{\rm adiab}$ (MeV)	$B_{\rm Bass}$ (MeV)
^{40}Ca+ ^{48}Ca	[6]	0.62	48.2±0.3	46.7	51.7
^{28}Si+ ^{64}Ni	[9]	0.70	48.4±0.3	47.6	50.8
^{30}Si+ ^{64}Ni	[9]	0.66	48.6±0.3	47.4	50.2
^{40}Ca+ ^{44}Ca	[6]	0.64	48.7±0.3	48.2	52.6
^{30}Si+ ^{62}Ni	[9]	0.66	49.0±0.3	48.2	50.6
^{28}Si+ ^{62}Ni	[9]	0.69	49.1±0.3	48.6	51.1
^{30}Si+ ^{58}Ni	[9]	0.67	49.7±0.3	49.3	51.2
^{40}Ca+ ^{40}Ca	[6]	0.65	50.2±0.2	50.6	53.5
^{28}Si+ ^{58}Ni	[9]	0.69	50.5±0.3	50.4	51.8
^{40}Ca+ ^{50}Ti	[13]	0.55	53.7±0.3	52.3	57.4
^{40}Ca+ ^{48}Ti	[13]	0.56	54.1±0.3	53.0	57.8
^{36}S+ ^{64}Ni	[9]	0.53	54.3±0.2	52.5	56.9
^{34}S+ ^{64}Ni	[9]	0.54	54.3±0.2	53.0	57.5
^{32}S+ ^{64}Ni	[9]	0.57	54.3±0.2	53.1	58.1
^{40}Ca+ ^{46}Ti	[13]	0.56	54.4±0.3	53.9	58.3
^{36}S+ ^{58}Ni	[9]	0.53	55.4±0.2	54.1	58.0
^{34}S+ ^{58}Ni	[9]	0.55	56.2±0.2	55.3	58.6
^{32}S+ ^{58}Ni	[9]	0.56	57.1±0.2	56.3	59.2
^{36}S+ ^{96}Zr	[15]	0.35	72.0±0.3	70.7	79.3
^{36}S+ ^{90}Zr	[15]	0.34	74.3±0.3	73.2	80.3
^{32}S+ ^{110}Pd	[11]	0.33	80.4±0.2	79.5	92.3
^{36}S+ ^{110}Pd	[11]	0.30	81.5±0.2	80.1	90.5
^{40}Ca+ ^{96}Zr	[12]	0.27	87.5±0.3	84.9	100.8
^{64}Ni+ ^{64}Ni	[5]	0.23	89.5±0.3	86.0	98.1
^{58}Ni+ ^{64}Ni	[5]	0.24	90.0±0.3	87.5	100.0
^{58}Ni+ ^{60}Ni	[10]	0.24	92.5±0.3	90.5	101.3
^{40}Ca+ ^{90}Zr	[12]	0.26	92.7±0.6	89.7	102.2
^{58}Ni+ ^{58}Ni	[4]	0.24	93.8±0.3	91.8	102.0
^{40}Ar+ ^{122}Sn	[7]	0.22	97.5±0.4	95.4	109.7
^{40}Ar+ ^{116}Sn	[7]	0.22	98.2±0.4	96.9	110.9
^{40}Ar+ ^{112}Sn	[7]	0.23	98.9±0.4	98.2	111.7
^{64}Ni+ ^{74}Ge	[5]	0.19	99.0±0.3	96.1	111.3
^{58}Ni+ ^{74}Ge	[5]	0.20	99.9±0.3	97.2	113.4
^{40}Ca+ ^{124}Sn	[14]	0.20	106.7±0.4	102.4	123.4
^{40}Ca+ ^{116}Sn	[14]	0.20	108.4±0.8	106.6	125.2
^{34}S+ ^{168}Er	[16]	0.21	111.2±0.5	112.4	130.2
^{40}Ar+ ^{154}Sm	[7]	0.18	112.3±0.4	113.6	133.3
^{40}Ar+ ^{148}Sm	[7]	0.18	116.9±0.4	116.2	134.5
^{40}Ar+ ^{144}Sm	[7]	0.18	119.3±0.4	118.3	135.4
^{86}Kr+ ^{76}Ge	[8]	0.14	123.1±0.4	119.6	139.7
^{86}Kr+ ^{70}Ge	[8]	0.14	123.8±0.4	119.9	141.9
^{40}Ca+ ^{192}Os	[3]	0.13	153.2±0.5	147.0	180.4
^{86}Kr+ ^{100}Mo	[8]	0.090	157.9±0.4	152.3	180.7
^{40}Ca+ ^{194}Pt	[3]	0.12	160.6±0.5	152.7	185.4
^{86}Kr+ ^{92}Mo	[8]	0.091	162.6±0.4	154.9	183.9
^{86}Kr+ ^{104}Ru	[8]	0.085	165.1±0.4	159.0	189.1
^{86}Kr+ ^{102}Ru	[8]	0.085	166.5±0.4	159.7	189.9
^{86}Kr+ ^{99}Ru	[8]	0.085	167.5±0.4	160.6	191.1
^{40}Ca+ ^{238}U	[17]	0.11	168±2[a]	170.3	213.0
^{48}Ca+ ^{208}Pb	[18]	0.10	169±2[a]	166.5	187.4
^{48}Ca+ ^{238}U	[18]	0.090	182±2[a]	178.2	206.9
^{58}Fe+ ^{208}Pb	[18]	0.066	217±2[a]	208.4	244.9

[a]Energy threshold for capture reaction.

and the number of protons $Z=Z_1+Z_2$. Calculating the liquid-drop-model contact force, we scale the radii R_1 and R_2 of the two nuclei as $r_0A_{1,2}^{1/3}$, allowing for some fine-tuning of the value of the r_0 parameter in order to obtain the best agreement with experimental data, and we then keep this value fixed for all nuclear systems. The ''effective'' radius parameter r_0, optimized in such a way, was found to be $r_0=1.15$ fm, a value that can be associated with the nuclear ''equivalent sharp radius'' [24].

Having determined the parameters of the nuclear part of the adiabatic fusion potential, Eq. (2), a comment should be made on the meaning of variable r in this one-dimensional potential. For large values $r>R_0$, its interpretation is clear: r can be identified with the distance between centers of the two nuclei. However, for $r<R_0$ where fusion proceeds through a sequence of shapes involving, e.g., formation of neck between the two fragments [25], the variable r becomes an effective (not well-defined) distance variable *along* the trajectory in the deformation space leading from the configuration of two nuclei in contact ($r=R_1+R_2$) to the equilibrium shape of the compound nucleus ($r=0$). Fortunately, the fusion barriers are located in the outer region $r>R_0$, where the variable r is clearly defined.

B. Coulomb potential

For typical applications, such as determination of the fusion barrier, it is sufficient to consider the Coulomb potential only in the outer region $r>R_0$, where the point-charge approximation gives sufficient accuracy

$$V_c(r)=\frac{Z_1Z_2e^2}{r}. \tag{7}$$

For completeness, in the inner region $r<R_0$ we propose to use a simple one-dimensional parametrization which joins the known values of the Coulomb energy in the contact configuration $V_c(r=R_0)=Z_1Z_2e^2/R_0$, with that of the equilibrium shape $V_c(r=0)=C_{cn}-C_1-C_2=C_0$. Using for this purpose the shape of the Fermi function which is consistent with the parametrization of the nuclear potential $V_n(r)$, and requiring continuity of the Coulomb potential and its derivative at $r=R_0$, we obtain for $r<R_0$

$$V_c(r)=k_1+\frac{k_2}{1+\exp\left(\dfrac{r-R_0}{a_c}\right)}, \tag{8}$$

where $k_1=2C_{R0}-C_0$, $k_2=2C_0-2C_{R0}$, and $a_c=R_0(C_0-C_{R0})/2C_{R0}$. In these expressions, $C_{R0}=Z_1Z_2e^2/R_0$ and C_0 is defined by Eq. (4). The sum of the nuclear potential (2) and the Coulomb potential (7),(8) gives the dependence of the total potential energy of a nucleus-nucleus system on the distance variable r, thus determining the height of the fusion barrier.

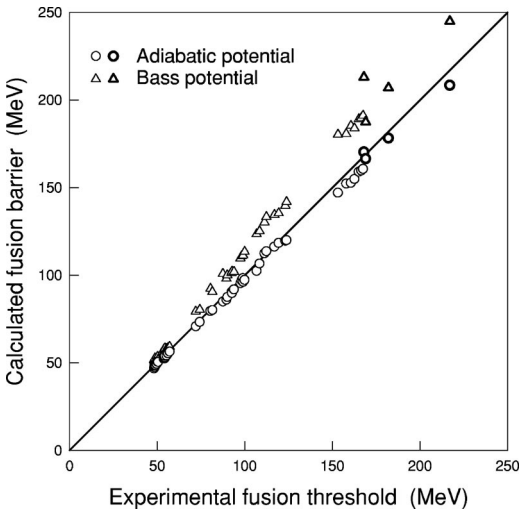

FIG. 2. Fusion barriers calculated with the adiabatic fusion potential (circles) and with the Bass potential (triangles), compared with the fusion energy thresholds deduced from measured fusion [3–18] and capture [17,18] excitation functions. Results for capture reactions are marked by thick-edge symbols.

IV. EXPERIMENTAL FUSION THRESHOLDS VS ADIABATIC BARRIERS

As was discussed above, the nucleus-nucleus potential proposed in the previous section is expected to describe the adiabatic evolution of the system towards fusion, characterized by the lowest possible barrier. Therefore, we compare the experimental fusion thresholds, determined in Sec. II and listed in Table I, with our theoretical adiabatic barriers $B_{\rm adiab}$ defined by the condition $d(V_n+V_c)/dr=0$. The calculated fusion barriers $B_{\rm adiab}$ are listed in Table I and compared with the experimental fusion energy thresholds $E_{\rm thr}$ in Fig. 2. It is seen from this figure that there is a very good correlation between the thresholds $E_{\rm thr}$ and the adiabatic barriers $B_{\rm adiab}$, especially for medium-weight systems with $E_{\rm thr}$ below 100 MeV. For heavy systems, a good correlation between both quantities still remains, although a clear, systematic effect of an increasing difference $E_{\rm thr}-B_{\rm adiab}$ with increasing barrier height is observed. This effect is discussed in Sec. V.

For comparison, barrier heights calculated for the frequently used Bass potential [26] are also shown in Fig. 2. They are much higher than the experimental fusion thresholds, the obvious consequence of the fact that the Bass potential is not adiabatic, but on the contrary, constructed for frozen shapes of the colliding nuclei and thus giving relatively high values of unrelaxed interaction barriers. Consequently, the fusion barriers predicted with the Bass potential should be correlated with the upper part of the fusion barrier distributions rather than with the fusion thresholds. Therefore, the gap in Fig. 2 between predictions of the adiabatic potential and the Bass potential can be associated with the range of the barrier distributions deduced from the fusion-barrier excitation functions.

It is important to note that the correlation between the

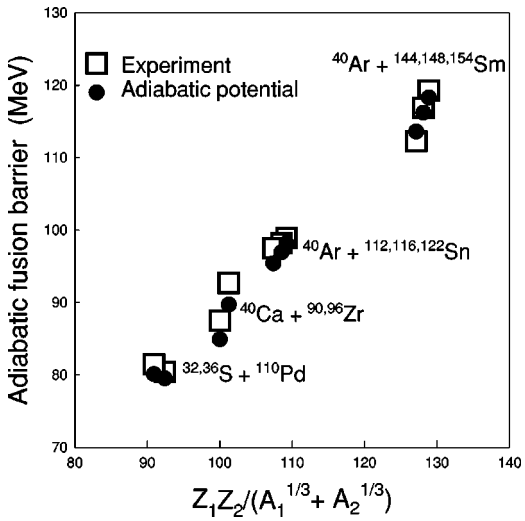

FIG. 3. Comparison of experimental fusion energy thresholds $E_{\rm thr}$ with calculated adiabatic fusion barriers for selected reactions with distinct isotopic effects, manifested by deviations from smooth dependence of the barrier height on $Z_1Z_2/(A_1^{1/3}+A_2^{1/3})$.

experimental fusion thresholds and Bass fusion barriers is worse than in the case of the adiabatic barriers: the points calculated with the Bass potential are more scattered in Fig. 2, and do not show such a regular linear dependence as the points corresponding to the adiabatic barriers. It is very likely that this difference results from the nuclear-structure (isotopic) effects which are not accounted for in the Bass potential, while present in the adiabatic potential.

We remind here that the depth of the nuclear part of the adiabatic potential V_0 depends on the ground-state masses of the two nuclei undergoing fusion, see Eq. (3). Essential structural properties of the nuclei (shell effects, deformation energy, isospin, etc.), which are included in the nuclear masses, obviously influence the height of the fusion barrier when the structural effects ''dissolve'' during the transition from the dinuclear to mononuclear configuration. As it is seen from Eq. (5), the diffuseness parameter a, related to V_0, also depends on the ground-state masses of the fusing nuclei. This additionally amplifies the modulation of the adiabatic fusion barrier by structural properties of the nuclei undergoing fusion.

The effect of nuclear structure is illustrated in Fig. 3. Experimental values of $E_{\rm thr}$ for several groups of reactions with distinct isotopic effects have been plotted as a function of $Z_1Z_2/(A_1^{1/3}+A_2^{1/3})$, the quantity that should precisely scale fusion barriers in the absence of nuclear structure. However, due to the isotopic effects, the experimental $E_{\rm thr}$ values evidently show irregular deviations from the expected smooth, nearly linear dependence on $Z_1Z_2/(A_1^{1/3}+A_2^{1/3})$. It is seen from Fig. 3 that the barrier heights calculated with the adiabatic potential closely follow all these irregularities. This result indicates that the nuclear structure effects are accounted for in the adiabatic potential quite well.

V. CAPTURE ENERGY THRESHOLDS FOR VERY HEAVY SYSTEMS

Very good correlation between the experimental fusion thresholds and the adiabatic fusion barriers gives a possibility of using this correlation for predictions of the energy thresholds for very heavy systems for which fusion cross sections cannot be reliably measured. We should note, however, that in case of very heavy systems, the fact of overcoming the entrance barrier does not guarantee formation of the compound nucleus because the system may reseparate along the fission valley. Thus, referring to the process in which such a heavy system overcomes the barrier, we should use the term ''capture cross section'' instead ''fusion cross section.'' After being captured, the combined system may either fuse or reseparate undergoing a fissionlike process, frequently called ''fast fission.''

With the aim to predict the capture cross sections for very heavy systems, in our compilation we have included results for four heavy systems, for which capture excitation functions had been measured [17,18] at near-threshold energies allowing the determination of the capture energy thresholds by using the same criterion of Eq. (1) as in the analysis of the fusion reactions. The capture energy thresholds and the corresponding adiabatic barriers for the ^{40}Ca+ ^{238}U, ^{48}Ca + ^{208}Pb, ^{48}Ca+ ^{238}U, and ^{58}Fe+ ^{208}Pb systems are listed in Table I. They are also shown in Fig. 2, marked with different symbols. It is seen from Fig. 2 that the correlation between $E_{\rm thr}$ and $B_{\rm adiab}$ established for fusion reactions, naturally extends to the domain of capture processes in collisions of very heavy systems.

As mentioned previously, for very heavy systems, the calculated adiabatic barriers $B_{\rm adiab}$ are smaller than the experimental fusion thresholds $E_{\rm thr}$. (The circles representing large values of $B_{\rm adiab}$ lay in Fig. 2 below the diagonal.) We interpret this difference as the ''extra-push'' energy [27], i.e., an excess of kinetic energy above the top of the interaction barrier that is necessary in order to overcome the barrier and achieve fusion (avoiding reseparation of the system). To verify this hypothesis, we calculated realistic fusion trajectories for several systems using the code HICOL based on the classical dynamical model with one-body dissipation, proposed by Feldmeier [28]. In these simulations, a trajectory at the lowest possible energy still leading to fusion was calculated for central collisions ($l=0$). To give some examples: the excess of kinetic energy $E_{\rm extra}$, necessary to overcome the highest point of the potential energy along this ''first-fusing'' trajectory was found to be only 1.0 MeV for the ^{40}Ca+ ^{90}Zr system, but already 6.3 MeV for a considerably heavier ^{40}Ca+ ^{194}Pt system. An essential part of the extra push energy can be attributed to the dissipative loss of kinetic energy during the approach to the top of the interaction barrier, and the remaining part of it is an excess of kinetic energy at the top of the barrier, necessary to avoid reseparation. The calculated values of the extra push energy agree with the average trend in the observed differences $E_{\rm thr}-B_{\rm adiab}$.

By averaging the differences $E_{\rm extra}=E_{\rm thr}-B_{\rm adiab}$, we found that $E_{\rm extra}$ can be approximated by

$$E_{\rm extra}=0.12B_{\rm adiab}-12\ \ {\rm MeV}\quad {\rm for}\quad B_{\rm adiab}>100\ \ {\rm MeV},$$

$$E_{\rm extra}=0\quad {\rm for}\quad B_{\rm adiab}\leqslant 100\ \ {\rm MeV}. \qquad (9)$$

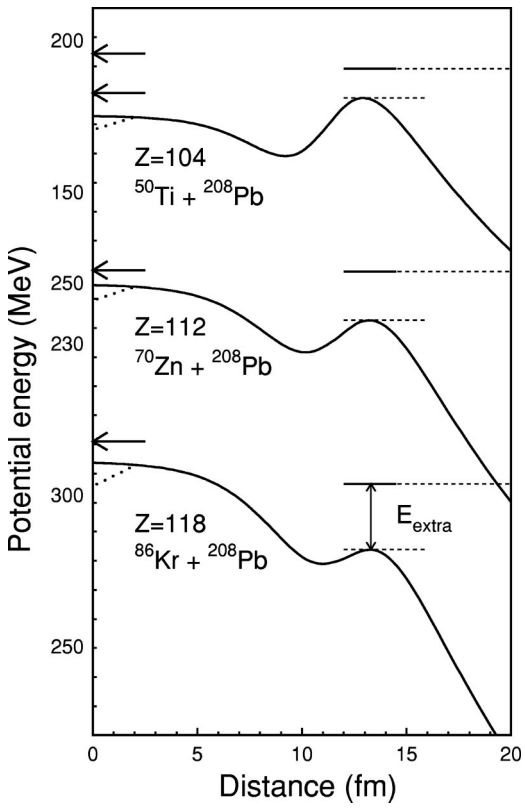

FIG. 4. Fusion potential energy curves for the ^{50}Ti $+ ^{208}$Pb, ^{70}Zn$+ ^{208}$Pb, and ^{86}Kr$+ ^{208}$Pb reactions, in which new elements of $Z=104$, 110, and 118, respectively, were synthesized [29,30]. Solid lines represent the nuclear plus Coulomb potential given by Eqs. (2)–(6) and (7), (8), respectively. The effect of the shell correction energy S_{cn}, which is assumed to vanish at the saddle point, is indicated by dotted lines. (See text.)

This simple expression fits the observed differences $E_{\rm thr} - B_{\rm adiab}$ and also agrees with the general trend in magnitudes of the extra push energies calculated with the code HICOL. Therefore, Eq. (9) can be used for correcting predictions of fusion energy thresholds $E_{\rm thr}=B_{\rm adiab}+E_{\rm extra}$, when precise experimental information on the fusion excitation function is not available. We propose to use the same correction given by Eq. (9) also for capture reactions, in spite of the fact that the extra push energy cannot be clearly defined and predicted in the dynamical model calculations for this class of reactions.

Predictions of the fusion-potential energy for very heavy nuclear systems used for production of superheavy elements are shown in Fig. 4. Displayed are results of calculations for the ^{50}Ti$+ ^{208}$Pb and ^{70}Zn$+ ^{208}$Pb reactions used at GSI Darmstadt to produce elements $Z=104$ and $Z=112$, respectively [29], and for the ^{86}Kr$+ ^{208}$Pb reaction used at LBNL Berkeley [30] to synthesize the $Z=118$ element. Experiments with these nuclear systems were carried out at the bombarding energies, at which the expected excitation energy of the compound nucleus does not exceed 14 MeV thus ensuring the ''cold fusion'' process characterized by evaporation of only one neutron from the compound nucleus. (The bombarding energies are indicated in Fig. 4 by horizontal arrows. For $Z=104$, two arrows are drawn, indicating the range of bombarding energies at which the ''cold fusion'' reaction was observed.) We should remember that the potential energy curves shown in Fig. 4 represent a simplified one-dimensional trace of the fusion trajectory in a more complex multidimensional space. In this one-dimensional presentation, the conventional saddle point, leading a trajectory to fusion, is represented by a maximum near the compound nucleus configuration. The maximum is formed only due to shell effects which quickly vanish with increasing deformation (or ''distance'' in notation on Fig. 4). Without shell effects there is no minimum at the equilibrium shape for so heavy composite systems.

The calculated fusion-potential curves illustrate a tendency characteristic for very heavy systems: contrary to lighter systems, the potential energy of the compound nucleus is raised to a level comparable or even higher than the height of the entrance-channel Coulomb barrier and therefore the apparent well in the potential energy behind the barrier becomes very shallow.

The adiabatic barriers shown in Fig. 4, corrected for the energy $E_{\rm extra}$ needed to overcome the barrier, represent the predicted values of the fusion energy threshold $E_{\rm thr}$ at which we know approximately the fusion cross section or, for very heavy systems, the capture cross section $\sigma_{\rm cap}(E_{\rm thr})\approx\pi\lambda\!\!\!^{-2}$. As it is seen from Fig. 4, for $Z=118$, $E_{\rm thr}$ is already below the saddle-point energy. Myers and Świątecki [31,32] suggested that this effect of ''unshielding'' the saddle point explains why the cross section for the production of the $Z=118$ element turned out to be enhanced with respect to the extremely low value predicted from extrapolation of the exponential trend observed for lighter elements of $102\leqslant Z\leqslant 112$. According to Refs. [31,32], only due to this unexpected enhancement factor, could the new element $Z=118$ have been successfully produced.

However, in our opinion, the completely unshielded reactions, such as in case of the ^{86}Kr$+ ^{208}$Pb system, do not directly guarantee an enhancement of the cross section for the compound-nucleus formation. The lowering of the entrance barrier with respect to the saddle-point energy can only increase the capture cross section, but this effect is probably counteracted by the decreasing probability of the transition of the dinuclear composite system into the compound nucleus. This expectation follows from the dynamical model calculations assuming the strong one-body dissipation. Such calculations show that the available kinetic energy is almost immediately thermalized once the interaction barrier is passed. Consequently, further radial motion towards fusion is stopped, and in order to fuse, the system must climb and overcome the saddle stochastically.

Our joint work along these lines with Świątecki led us to the conviction that realistic estimates of the capture cross sections, combined with the concept of thermal fluctuations governing the transition of the ''clutched'' composite system into the compound nucleus, pave the way for reasonable quantitative estimates of the cross sections for production of new superheavy elements.

ACKNOWLEDGMENTS

We would like to thank W. J. Świątecki for many inspiring discussions. We are grateful to A. M. Stefanini for sending us some unpublished tabulated data on fusion excitation functions and M.G. Itkis for providing us with unpublished data on the capture cross sections for the heaviest systems. This work was supported by the Poland-U.S.A. Maria Skłodowska-Curie Joint Fund II, under Project No. PAA/DOE-98-34, and by the Polish State Committee of Scientific Research, KBN, Grant No. 2P03B05419.

[1] M. Dasgupta, D. J. Hinde, N. Rowley, and A. M. Stefanini, Annu. Rev. Nucl. Part. Sci. **48**, 401 (1998).
[2] N. Rowley, G. R. Satchler, and P. H. Stelson, Phys. Lett. B **254**, 25 (1991).
[3] J. D. Bierman, P. Chan, J. F. Liang, M. P. Kelly, A. A. Sonzogni, and R. Vandenbosch, Phys. Rev. C **54**, 3068 (1996).
[4] M. Beckerman, M. Salomaa, A. Sperduto, H. Enge, J. Ball, A. DiRienzo, S. Gazes, Yan Chen, J. D. Molitoris, and Mao Naifeng, Phys. Rev. Lett. **45**, 1472 (1980).
[5] M. Beckerman, M. Salomaa, A. Sperduto, J. D. Molitoris, and A. DiRienzo, Phys. Rev. C **25**, 837 (1982).
[6] H. A. Aljuwair, R. J. Ledoux, M. Beckerman, S. B. Gazes, J. Wiggins, E. R. Cosman, R. R. Betts, S. Saini, and Ole Hansen, Phys. Rev. C **30**, 1223 (1984).
[7] W. Reisdorf, F. P. Hessberger, K. D. Hildebrand, S. Hofmann, G. Münzenberg, K.-H. Schmidt, J. H. R. Schneider, W. F. W. Schneider, K. Sümmerer, G. Wirth, J. V. Kratz, and K. Schlitt, Nucl. Phys. **A438**, 212 (1985).
[8] W. Reisdorf, F. P. Hessberger, K. D. Hildebrand, S. Hofmann, G. Münzenberg, K.-H. Schmidt, W. F. W. Schneider, K. Sümmerer, G. Wirth, J. V. Kratz, K. Schlitt, and C.-C. Sahm, Nucl. Phys. **A444**, 154 (1985).
[9] A. M. Stefanini, G. Fortuna, R. Pengo, W. Meczynski, G. Montagnoli, L. Corradi, A. Tivelli, S. Beghini, C. Signorini, S. Lunardi, M. Morando, and F. Soramel, Nucl. Phys. **A456**, 509 (1986).
[10] A. M. Stefanini, D. Ackermann, L. Corradi, D. R. Napoli, C. Petrache, P. Spolaore, P. Bednarczyk, H. Q. Zhang, S. Beghini, G. Montagnoli, L. Mueller, F. Scarlassara, G. F. Segato, F. Soramel, and N. Rowley, Phys. Rev. Lett. **74**, 864 (1995).
[11] A. M. Stefanini, D. Ackermann, L. Corradi, J. H. He, G. Montagnoli, S. Beghini, F. Scarlassara, and G. F. Sagato, Phys. Rev. C **52**, R1727 (1995).
[12] H. Timmers, D. Ackermann, S. Beghini, L. Corradi, J. H. He, G. Montagnoli, F. Scarlassara, A. M. Stefanini, and N. Rowley, Nucl. Phys. **A633**, 421 (1998).
[13] A. A. Sonzogni, J. D. Bierman, M. P. Kelly, J. P. Lestone, J. F. Liang, and R. Vandenbosch, Phys. Rev. C **57**, 722 (1998).
[14] F. Scarlassara, S. Beghini, G. Montagnoli, G. F. Segato, D. Ackermann, L. Corradi, C. J. Lin, A. M. Stefanini, and L. F. Zheng, Nucl. Phys. **A672**, 99 (2000).
[15] A. M. Stefanini, L. Corradi, A. M. Vinodkumar, Yang Feng, F. Scarlassara, G. Montagnoli, S. Beghini, and M. Bisogno, Phys. Rev. C **62**, 014601 (2000).
[16] C. R. Morton, A. C. Berriman, R. D. Butt, M. Dasgupta, A. Godley, D. J. Hinde, and J. O. Newton, Phys. Rev. C **62**, 024607 (2000).
[17] W. Q. Shen, J. Albinski, A. Gobbi, S. Gralla, K. D. Hildenbrand, N. Hermann, J. Kuzminski, W. F. J. Müller, H. Stelzer, J. Tōke, B. B. Back, S. Bjørnholm, and S. P. Sørensen, Phys. Rev. C **36**, 115 (1987).
[18] M. G. Itkis, Yu. Ts. Oganessian, E. M. Kozulin, A. A. Bogatchev, I. M. Itkis, M. Jandel, J. Kliman, G. N. Kniajeva, N. A. Kondratiev, I. V. Korzyukov, L. Krupa, I. V. Pokrovski, V. A. Ponomarenko, E. V. Prokhorova, A. Ya. Rusanov, V. M. Voskresenski, F. Hanappe, B. Benoit, T. Materna, N. Rowley, L. Stuttge, G. Giardina, and K. J. Moody, in *Proceedings of the International Workshop on Fusion Dynamics at the Extremes*, Dubna, Russia, 2000 (World Scientific, Singapore, in press).
[19] J. Wilczyński and K. Siwek-Wilczyńska, Phys. Lett. **55B**, 270 (1975).
[20] K. Siwek-Wilczyńska and J. Wilczyński, Phys. Lett. **74B**, 313 (1978).
[21] W. D. Myers and W. J. Swiatecki, Ark. Fys. **36**, 343 (1967).
[22] P. Möller, J. R. Nix, W. D. Myers, and W. J. Świątecki, At. Data Nucl. Data Tables **59**, 185 (1995).
[23] J. Wilczyński, Nucl. Phys. **A216**, 386 (1973).
[24] W. D. Myers, Nucl. Phys. **A204**, 465 (1973).
[25] J. Błocki and W. J. Świątecki, Report No. LBL-12811, Berkeley, 1982 (unpublished).
[26] R. Bass, Nucl. Phys. **A231**, 45 (1974).
[27] W. J. Swiatecki, Nucl. Phys. **A376**, 275 (1982).
[28] H. Feldmeier, Rep. Prog. Phys. **50**, 915 (1987).
[29] S. Hofmann, Rep. Prog. Phys. **61**, 639 (1998).
[30] V. Ninov, K. E. Gregorich, W. Loveland, A. Ghiorso, D. C. Hoffman, D. M. Lee, H. Nitsche, W. J. Swiatecki, U. W. Kirbach, C. A. Laue, J. L. Adams, J. B. Patin, D. A. Shaughnessy, D. A. Strellis, and P. A. Wilk, Phys. Rev. Lett. **83**, 1104 (1999).
[31] W. D. Myers and W. J. Świątecki, Phys. Rev. C **62**, 044610 (2000).
[32] W. D. Myers and W. J. Świątecki, Acta Phys. Pol. B **32**, 1033 (2001).